

Scaling of the Non-Phononic Spectrum of Two-Dimensional Glasses

Lijin Wang^{1,*}, Grzegorz Szamel², and Elijah Flenner^{2,†}

¹School of Physics and Optoelectronic Engineering, Anhui University, Hefei 230601, China

²Department of Chemistry, Colorado State University, Fort Collins, Colorado 80523, USA

* Corresponding author, Email: lijin.wang@ahu.edu.cn

† Corresponding author, Email: flenner@gmail.com

(Dated: May 6, 2023)

Low-frequency vibrational harmonic modes of glasses are frequently used to rationalize their universal low-temperature properties. One well studied feature is the excess low-frequency density of states over the Debye model prediction. Here we examine the system size dependence of the density of states for two-dimensional glasses. For systems of fewer than 100 particles, the density of states scales with the system size as if all the modes were plane-wave-like. However, for systems greater than 100 particles we find a different system-size scaling of the cumulative density of states below the first transverse sound mode frequency, which can be derived from the assumption that these modes are quasi-localized. Moreover, for systems greater than 100 particles, we find that the cumulative density of states scales with frequency as a power law with the exponent that leads to the exponent $\beta = 3.5$ for the density of states. For systems sizes investigated we do not see a size-dependence of exponent β .

A striking feature of glasses is the excess of low-frequency vibrational harmonic modes over that predicted by Debye theory. Many computational studies analyzed low-frequency vibrational modes in glasses [1–4] with the goal to characterize the excess harmonic modes, which are frequently referred to as non-phononic modes. Since the same low-temperature properties are found in different glasses, one is naturally tempted to look for universal features of the excess modes, independent of the model and the glass formation protocol. Importantly, these features should hold in the thermodynamic limit. In many studies the implicit hypothesis is that the excess modes density $\mathcal{D}_{ex}(\omega)$ follows a power law, $\mathcal{D}_{ex}(\omega) = A_{ex}\omega^\beta$.

Different methods in the literature are employed to determine β . One approach is to separate modes by their participation ratio with the assumption that the low-frequency excess modes have a significantly smaller participation ratio than the extended, plane-wave-like modes [5–7]. This method was used to argue that $\beta = 4$ in three dimensions [6, 7]. However, this method fails in two dimensions since it is impossible to choose a suitable participation ratio cutoff to differentiate between the excess modes and the plane-wave-like modes in two dimensions.

A second method is to study small systems [8–10]. In d spatial dimensions the frequency range of the first band of plane-wave-like modes scales as $L^{-d/2}$ where L is the simulation box size. The assumption is that the modes below this band of plane-wave-like modes represent the excess modes and one can determine the scaling of $\mathcal{D}_{ex}(\omega)$ from studying the harmonic mode spectrum for frequencies significantly below those of the first band. While conceptually straight forward, there are some subtle issues that must be kept in mind. First, every simulated glass has a slightly different shear modulus that results in a slightly different frequency expected for the first plane-wave-like mode, ω_{T1} , for an ideal elastic body. In addition, the modes are not pure plane waves and there is

a distribution of frequencies around ω_{T1} for each glass. For these reasons one can have a rather large range of frequencies where the first plane-wave-like modes exist. If one does not separate the plane-wave-like modes (like in the first method), one has to be careful to infer $\mathcal{D}_{ex}(\omega)$ using only modes that do not correspond to plane-wave-like modes.

Another difficulty is that there is a reported finite size effect influencing the exponent β in three-dimensional glasses [10]. It has been reported that $\beta < 4$ for small systems and β equals 4 for large enough systems [10]. Recall that the plane-wave-like modes move to lower frequencies with increasing system size, and thus there is a smaller frequency range where the excess modes spectrum is found. In addition, in two dimensions there are very few excess modes [7, 11] and a very large number of glass realizations are needed to obtain good enough statistics to determine an accurate value for β . Analysis of β in two dimensions is also complicated by a reported finite size effect in the pre-factor A_{ex} , $A_{ex} \sim (\log N)^{(\beta+1)/2}$ with N the number of particles in the system [9].

Finally, several groups attempted to disentangle or de-hybridize observed harmonic modes into plane-wave or phonon-like modes and localized modes [12–19]. For three-dimensional systems [12, 14], these methods result in $\beta = 4$, and thus agree with what has been found in studying small systems and from separating the modes by participation ratio. De-hybridization procedures also suggest that $\beta = 4$ for two-dimensional systems [18, 19]. Wang *et al.* [11] examined the scaling of the excess modes above ω_{T1} by subtracting the Debye contribution from the total cumulative density of states and found that the excess modes appeared to scale as ω^2 , which suggests a change of scaling of excess modes when quasi-localized modes and plane-wave modes hybridize. A change of the scaling of excess modes above ω_{T1} with hybridization was also suggested by Shiraishi *et al.* [19], resulting in the ex-

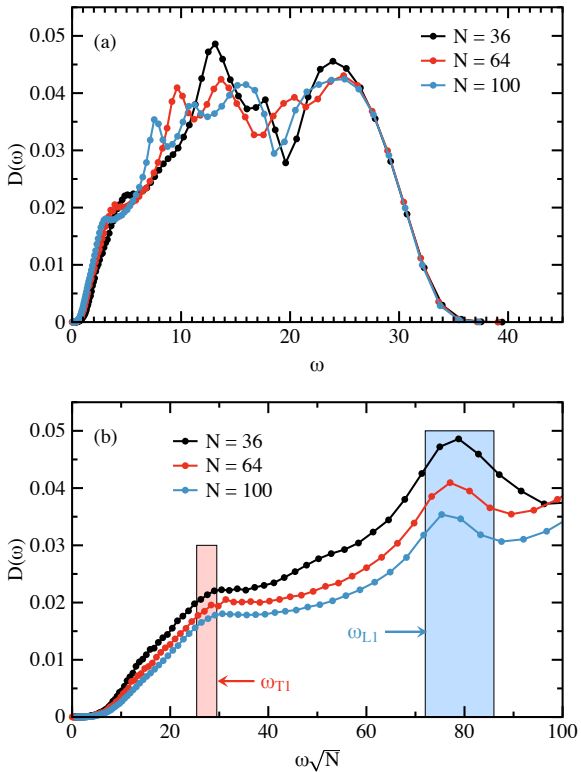


FIG. 1: (a) The density of states of small two-dimensional glasses with N particles. There is a distinct system size dependence with a shoulder at low frequencies and peaks showing up at N dependent frequencies. (b) The density of states versus $\omega\sqrt{N}$. The shoulder is shown to correspond to $\omega_{T1} = \sqrt{G/\rho}(2\pi/L)$ and the first peak corresponds to $\omega_{L1} = \sqrt{(G+K)/\rho}(2\pi/L)$. The shaded regions represent the range of ω_{T1} and ω_{L1} due to the range of bulk modulus and shear modulus calculated for the different glasses.

cess modes scaling as ω^3 . In contrast, excess modes above ω_{T1} in three dimensions scale as ω^4 [6, 7, 11].

A clear picture of the scaling of harmonic modes has not emerged in two-dimensional systems. In this work, in order to clarify the picture of harmonic vibrations in two-dimensional glasses we examine in detail the spectrum of harmonic modes below ω_{T1} and explore its finite size effects.

We present analysis of our results of the cumulative density of states $I(\omega) = \int_{0+}^{\omega} D(\omega') d\omega'$, where $D(\omega)$ is the full density of states. We emphasize that to avoid any binning algorithm-related issues we evaluate the cumulative distribution $I(\omega)$ directly, by counting the number of eigenfrequencies less than ω . We find power-law behavior implying $\beta \approx 3.5$ for systems greater than 100 particles. We also study in detail some finite size effects of the density of states observed in two-dimensional glasses and find different behavior for systems less than 100 particles and greater than 100 particles. In contrast to a recent paper [20], we do not see a system size dependence of exponent β , at least for the range of system sizes investigated.

For an ideal elastic body, the frequency of the first transverse wave is given by $\omega_{T1} = \sqrt{(G/\rho)(2\pi/L)}$, where G is the shear modulus, ρ is the mass density, and L is the linear size of the sample. The frequency of the first longitudinal wave is given by $\omega_{L1} = \sqrt{(G+K)/\rho}(2\pi/L)$, where K is the bulk modulus. We start our analysis of the IPL-10 system quenched from configurations equilibrated at parent temperature $T_p = 2.0$ that are discussed in Ref. [11]. Shown in Fig. 1 is the density of states $D(\omega) = (2N-2)^{-1} \sum_n \delta(\omega - \omega_n)$ for $N = 36, 64$, and 100 . The frequencies ω_n are obtained by diagonalizing the Hessian matrix. For these system sizes there are two distinct features at low frequencies, a shoulder and a peak. In Fig. 1(b) we scale the frequency by $\sqrt{N} \sim L$ and find that the two low frequency features align. The shaded regions represent the range of frequencies of ideal plane waves, ω_{T1} (red) and ω_{L1} (blue), which is derived from the range of values for G and K . Fig. 1(b) suggests that the shoulder is associated with the first transverse wave and the peak is associated with the first longitudinal wave.

To determine the scaling exponent of the density of states, β , we examine the cumulative density of states $I(\omega)$. Since the hypothesis is that the modes corresponding to the lowest frequencies below ω_{T1} are quasi-localized and contribute to $\mathcal{D}_{ex}(\omega)$, we should be able to infer $\mathcal{D}_{ex}(\omega)$ from the low frequency behavior of $I(\omega)$.

We examined the scaling of $I(\omega)$ for very small systems of $N \leq 100$ particles. Shown in Fig. 2(a) is $I(\omega)$ versus $\omega\sqrt{\log N}$, which is a scaling predicted from continuum elasticity due to a r^{-1} decay of the non-phononic modes at large distances r [9, 15]. There is a systematic deviation from this scaling. In contrast, we find nearly perfect data collapse of $I(\omega)[2N-2]$ versus $\omega\sqrt{N}$, Fig. 2(b), which is a scaling motivated by the system size dependence of Debye theory. We are counting the average number of modes up to $\omega\sqrt{N}$ and seeing how many fall below $\omega_{T1}\sqrt{N}$. For an ideal elastic body, $I(\omega)[2N-2] = 4$ at $\omega_{T1}\sqrt{N}$. The shaded area in Fig. 2(b) represents the range of ω_{T1} given the range of values for G . For these very small systems we do not find any evidence that there are more modes in excess of the Debye theory, and we do not believe that the excess mode scaling can be inferred from systems less than 100 particles. This analysis also highlights the difficulty in determining the frequency range to use to study excess (non-phononic) modes. We emphasize that while the observed scaling of the cumulative density of states with N agrees with the Debye theory, this fact does not imply that the modes are plane-wave-like. For these very small systems it is difficult to distinguish between plane-wave-like and quasi-localized modes.

We fit $I(\omega)[2N-2]$ versus $\omega\sqrt{N}$ for $3 \leq \omega\sqrt{N} \leq 6$ for $N = 36, 64$ and 100 to $a(\omega\sqrt{N})^{\beta+1}$. We find that β varies from 3.38 for $N = 36$ to 3.61 for $N = 64$, and that $\beta = 3.48$ for $N = 100$. We show the fits for $N = 36$ and $N = 64$ in Fig. 2(b). It is impossible to determine from the fits if one value of β should be preferred over another.

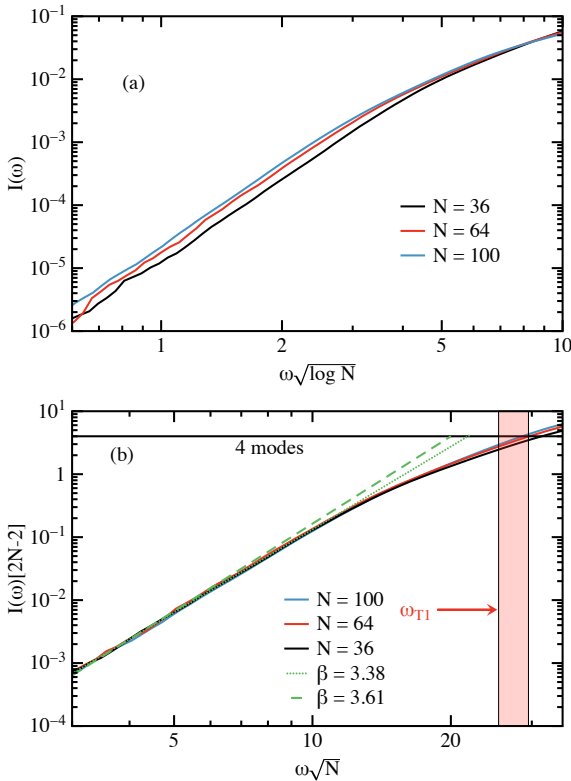


FIG. 2: (a) Scaling of the cumulative density of states proposed in Ref. [15]. There are small deviations from this scaling for these small system sizes. (b) Expected scaling of the cumulative density of states if all the modes are plane-wave-like. This scaling results in better data collapse than the scaling proposed in Ref. [15] for these small system sizes. The red shaded area is the typical range of frequencies $\omega_{T1}\sqrt{N}$ expected for an ideal transverse wave for the different glass configurations. For an ideal amorphous elastic body, $I(\omega)(2N - 2) = 4$ at ω_{T1} . The dotted green line is a fit to the $N = 36$ particle results and the dashed green line is a fit to the $N = 64$ particle results; the corresponding β in the fitting function $I(\omega)(2N - 2) \sim (\omega\sqrt{N})^{\beta+1}$ is indicated in the legend. Both fits are from $3 \leq \omega\sqrt{N} \leq 6$.

We find that this range of β is also consistent with the results of Ref. [20]. Ideally, we would want to greatly expand the fitting range to include at least one decade along each axis (*i.e.* at least one decade of ω and $I(\omega)$) to claim a specific power law, but finding a large range of frequencies in which a power law is obeyed requires many more independent configurations, that we cannot generate with our present computational resources. Here we are assuming a power law down to $\omega = 0$ and inferring β with the available data.

In contrast to our result for smaller systems, in Fig. 3(a) we show that the $I(\omega) = f(\omega\sqrt{\log N})$ scaling is obeyed for $100 < N \leq 30000$ [24]. Since the $f(\omega\sqrt{\log N})$ scaling is derived from continuum elasticity [9, 15], it is unsurprising that this scaling breaks down for small systems, see Fig. 2(a). This is also consistent with the work by Wittmer *et al.* [21] and Tanguy *et al.* [22] which

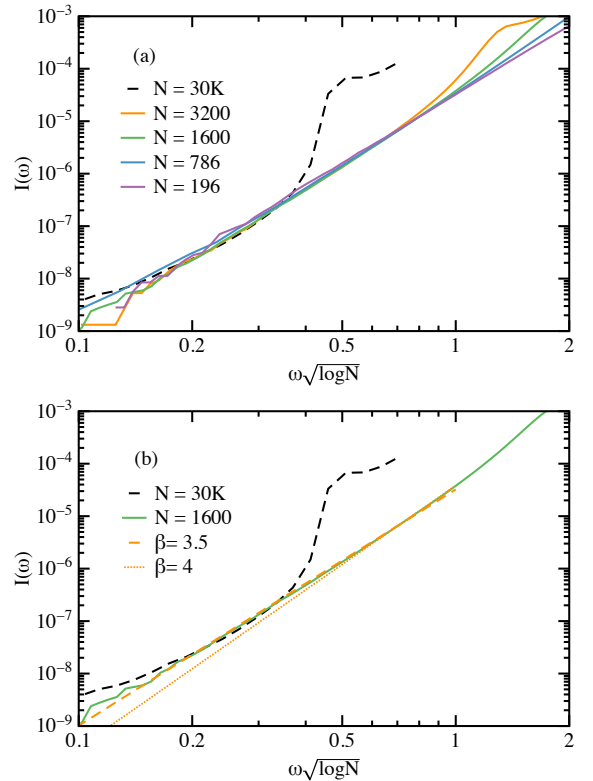


FIG. 3: (a) Scaling plot of the cumulative density of states for system sizes $196 \leq N \leq 30000$ for the IPL-10 system [11]. Unlike for smaller systems, the $I(\omega) = f(\omega\sqrt{\log N})$ scaling produces reasonable data collapse at small frequencies. There is some deviation at low frequencies, but this cannot be statistically ruled out. (b) Direct comparison for systems of $N = 1600$ and $N = 30000$. We fit the $N = 1600$ particle system from $0.2 \leq \omega\sqrt{\log N} \leq 0.8$ to $I(\omega\sqrt{\log N}) \sim (\omega\sqrt{\log N})^{\beta+1}$. The dotted orange line corresponds to a fit with $\beta = 4$ fixed, while the dashed orange line corresponds to a fit with $\beta = 3.5$ fixed.

concluded that continuum elasticity breaks down below about 30 particle diameters for 2D systems. There are some deviations from scaling at the smallest frequencies, but we believe that better statistics would improve the overlap. In Fig. 3(b) we show only the $N = 1600$ and $N = 30000$ results. We fit the $N = 1600$ results for $0.2 \leq \omega\sqrt{\log N} \leq 0.8$ to $I(\omega\sqrt{\log N}) \sim (\omega\sqrt{\log N})^{\beta+1}$ where we fixed $\beta = 4$ (orange dotted line) and $\beta = 3.5$ (orange dashed line). The $\beta = 3.5$ fit provides a better description of the $N = 30000$ results. Note that we cannot statistically rule out $\beta = 4$ on this analysis alone, but we will show that $\beta \approx 3.5$ is consistent with all our results for systems over 100 particles.

To investigate the effect of annealing on the value of β we studied systems of $N = 1600$ and $N = 30000$ particles. To anneal the samples we simulated each configuration for 10^6 time steps with a time step of 0.01 at $T = 0.5$ before quenching to $T = 0$, as was done in Ref. [20]. Shown in Fig. 4 is $I(\omega)$ versus $\omega\sqrt{\log N}$ for these annealed

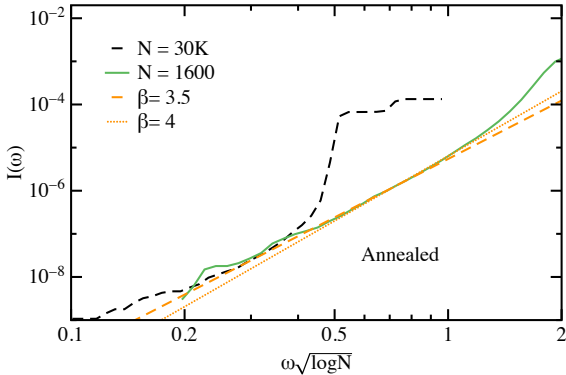


FIG. 4: Scaling plot of the cumulative density of states for annealed IPL-10 systems of $N = 1600$ and $N = 30\,000$. We fit the $N = 1600$ particle system to all the available data up to $\omega\sqrt{\log N} = 0.8$ to $I(\omega\sqrt{\log N}) \sim (\omega\sqrt{\log N})^{\beta+1}$. The dotted orange line corresponds to a fit with $\beta = 4$ fixed, while the dashed orange line corresponds to a fit with $\beta = 3.5$ fixed.

systems. Again we find the $I(\omega) = f(\omega\sqrt{\log N})$ scaling is obeyed. We fit the $N = 1600$ particle system using all the available data up to $\omega\sqrt{\log N} = 0.8$ where we fixed $\beta = 4$ (orange dotted line) and $\beta = 3.5$ (orange dashed line). We find that the $\beta = 3.5$ fit provides a better description of the data over a larger range of $\omega\sqrt{\log N}$ for the $N = 1600$ particle systems. The $\beta = 3.5$ fit describes $I(\omega)$ for the $N = 30\,000$ particle system for a range of ω , whereas the $\beta = 4$ fit does not. We conclude that the $\beta = 3.5$ provides a better description of the results for the annealed system also.

We recall that there was an outlier in the results shown in Ref. [11]. Figure 5 is a reproduction of Fig. 2(b) of the supplemental material of Ref. [11], which shows $I(\omega)/\omega^{4.5}$ (corresponding to $\beta = 3.5$) for the IPL-10 system for different system sizes. The low frequency data suggests that $\beta \approx 3.5$ for every system size except for $N = 786$. As pointed out in Ref. [20], the $N = 786$ particle result shows an upturn at small frequencies suggesting a β different than the other system sizes.

To address this result we increased the number of glass samples for this interaction potential and system size from the 0.79 million samples used in Ref. [11] to 2.4 million samples. Shown in Fig. 6 is $I(\omega)/\omega^{4.5}$ for $N = 786$ with the improved statistics. We can see that the upturn starts at lower ω , where the statistics are poor, and there is a larger range of ω where $\beta \approx 3.5$ is a reasonable description of the data. With the improved statistics we thus find that $N = 786$ system is consistent with other results.

We now turn to the analysis of exponents β for all the systems. To determine the exponent β for systems of more than 100 particles we fit $\log[I(\omega)] = (\beta+1)\log(\omega) + a$. For each system size we fit three to four frequency ranges to obtain β and average β obtained from these fits. The uncertainty is chosen to include each value of β for a given interaction potential and system size. We

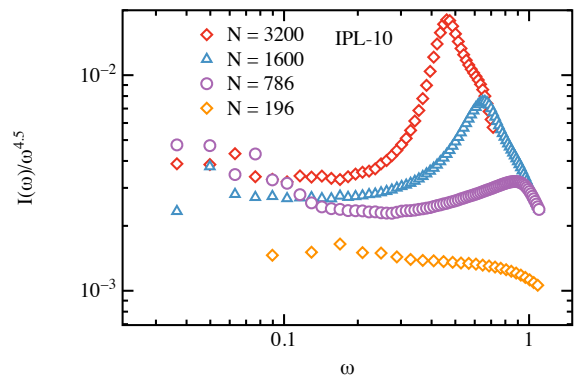


FIG. 5: The cumulative density of states for the IPL-10 system for different system sizes studied in Ref. [11]. Note that this figure is a reproduction of Fig. 2(b) of the supplemental material of Ref. [11].

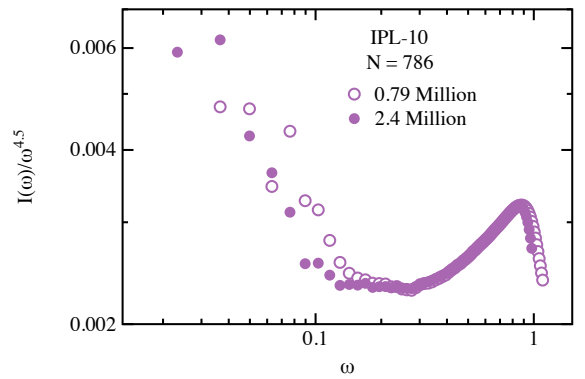


FIG. 6: Comparison of the scaled cumulative density of states for the IPL-10 system with $N=786$ for ensemble sizes of 0.79 million configurations (open symbols) and 2.4 million configurations (closed symbols).

exclude the results for the Lennard-Jones systems presented in Ref. [11] since there is a systematic downturn at small ω for each system size that is not seen for the other interaction potentials. Shown in Fig. 7 are the results for the remaining interaction potentials analyzed in Ref. [11] (closed symbols).

Figure 7 does not show any clear, systematic system size dependence of the exponent β , in contrast to the systematic change with system size suggested by the authors in Ref. [20]. For the harmonic sphere system (HARM), β does appear to grow with system size, but the growth is within the uncertainty of the calculation. The two inverse-power-law systems (IPL-10 and IPL-12) show no systematic change in β with system size.

We note that there are two values of β in Fig. 7 for the IPL-10 system with 786 particles. The filled circle was obtained from the original, smaller sample shown in Figs. 5 and 6. The open circle was obtained from the larger sample shown in Fig. 6. We note that with the improved statistics the value of exponent β is con-

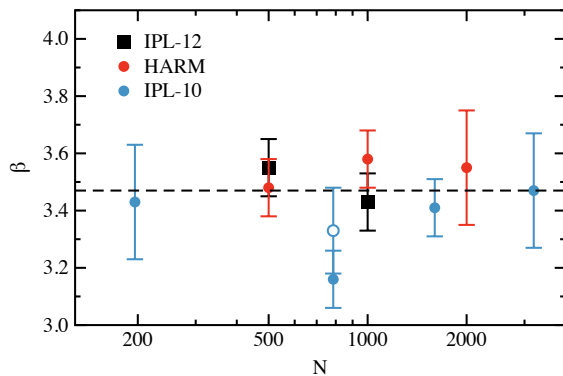


FIG. 7: The exponent β obtained from fits of the cumulative density of states $I(\omega)$ for the systems studied by Wang *et al.* in Ref. [11]. The horizontal line is the average value of β .

sistent with results for other system sizes. The change of β with increasing the number of glass samples highlights the difficulty of obtaining an accurate value of β for two-dimensional systems. There are so few excess modes that many glass samples are needed to obtain accurate results to do a direct calculation of the density of states. This was pointed out in Ref. [18] where the authors utilized non-linear mode analysis [16, 17] to analyze two-dimensional systems.

We find that all systems where $N > 100$ result in $\beta \approx 3.5$ for all our systems and we cannot rule out $\beta \approx 3.5$ for $N \leq 100$ with our data alone. We note that we do not believe that one can obtain the scaling of the non-phononic density of states for $N < 100$. We also find that $\beta \approx 3.5$ for systems greater than 100 particles is consistent with the data presented in Ref. [20].

All the systems discussed here are fairly small, and it is possible to study much larger systems. The difficulty with larger systems is that the first plane-wave-like modes get pushed to lower frequencies and the frequency range where only excess modes are expected to be found becomes smaller. This difficulty is combined with the very limited number of non-plane-wave-like modes in two-dimensions. We examined a 30 000 particle system for the same IPL-10 model as used in Ref. [11] and found inconclusive results for the value of β at the lowest frequencies examined, see Fig. 3(b). These results were

similar to those for three-dimensional systems in Ref. [23] in that β was smaller than 3.5 at lower frequencies. This puzzling result persisted despite having about 0.23 million configurations of 30 000 particles. Examination of these large systems deserves more work.

Here, as with much previous work, we are assuming that a power law is a good description of the low frequency modes despite not having several decades of frequency to verify that a power law does indeed exist. Having ensemble sizes large enough for a direct verification is a daunting task, especially for two-dimensional systems that have so few quasi-localized modes.

Two-dimensional solids and liquids have characteristics different than their three-dimensional counterparts [11, 25]. One characteristic for two-dimensional glasses is the very small density of excess modes, which makes studying the excess modes difficult. There is evidence that the density of the excess modes scales as ω^2 for excess modes above ω_{T1} for two-dimensional glasses [11], but the excess modes scale as ω^4 for three-dimensional glasses [11]. Two-dimensional glasses may be different than three or higher dimensions. Furthermore, since $\omega_{T1} \rightarrow 0$ in the thermodynamic limit, it is unclear that the scaling of the modes below ω_{T1} is important in the understanding of the behavior of two-dimensional glasses. Future work needs to focus on the influence of the scaling of excess harmonic modes on properties of glasses.

We thank E. Lerner and E. Bouchbinder for exhilarating discussions. We also thank E. Lerner and E. Bouchbinder for sharing some of their data published in Ref. [20], which we found to support the conclusions presented here. L. Wang acknowledges the support from National Natural Science Foundation of China (Grant No. 12004001), Anhui Projects (Grant Nos. 2022AH020009, S020218016 and Z010118169), Hefei City (Grant No. Z020132009), and Anhui University (start-up fund). E.F. and G.S. acknowledge support from NSF Grant No. CHE-2154241. We also acknowledge Hefei Advanced Computing Center, Beijing Super Cloud Computing Center, and the High-Performance Computing Platform of Anhui University for providing computing resources.

The authors have no conflicts to disclose. The data that support the findings of this study are available from the corresponding authors upon reasonable request.

[1] H. Mizuno and A. Ikeda, Phys. Rev. E **98**, 062612 (2018).
[2] L. Wang, L. Berthier, E. Flenner, P. Guan, and G. Szamel, Soft Matter **15**, 7018 (2019).
[3] E. Flenner, L. Wang, and G. Szamel, Soft Matter **16**, 775 (2020).
[4] G. Szamel and E. Flenner, J. Chem. Phys. **156**, 144502 (2022).
[5] H. R. Schober and B. B. Laird, Phys. Rev. B **44**, 6476 (1991).
[6] L. Wang, A. Ninarello, P. Guan, L. Berthier, G. Szamel, and E. Flenner, Nat. Commun. **10**, 26 (2019).
[7] H. Mizuno, H. Shiba, and A. Ikeda, Proc. Natl. Acad. Sci. U.S.A. **114**, E9767 (2017).
[8] E. Lerner, G. Düring, and E. Bouchbinder, Phys. Rev. Lett. **117**, 035501 (2016).
[9] G. Kapteijns, E. Bouchbinder, and E. Lerner, Phys. Rev. Lett. **121**, 055501 (2018).
[10] E. Lerner, Phys. Rev. E **101**, 032120 (2020).
[11] L. Wang, G. Szamel, and E. Flenner, Phys. Rev. Lett. **127**, 248001 (2021); Phys. Rev. Lett. **129**, 019901(E)

(2022).

[12] J. A. Giannini, D. Richard, M. L. Manning, and E. Lerner, Phys. Rev. E **104**, 044905 (2021).

[13] L. Angelani, M. Paoluzzi, G. Parisi, and G. Ruocco, Proc. Natl. Acad. Sci. **115**, 8700 (2018).

[14] K. Shiraishi, Y. Hara, and H. Mizuno, Phys. Rev. E **106**, 054611 (2022).

[15] E. Lerner and E. Bouchbinder, J. Chem. Phys. **148**, 214502 (2018).

[16] G. Kapteijns, D. Richard, and E. Lerner, Phys. Rev. E **101**, 032130 (2020).

[17] L. Gartner and E. Lerner, SciPost Phys. **1**, 016 (2016).

[18] E. Lerner and E. Bouchbinder, J. Chem. Phys. **155**, 200901 (2021).

[19] K. Shiraishi, H. Mizuno, and A. Ikeda, arXiv:2301.06225.

[20] E. Lerner and E. Bouchbinder, J. Chem. Phys. **157**, 166101 (2022).

[21] J. P. Wittmer, A. Tanguy, J.-L. Barrat, and L. Lewis, Europhys. Lett. **57**, 423 (2002).

[22] A. Tanguy, J. P. Wittmer, F. Leonforte, and J.-L. Barrat, Phys. Rev. B **66** 174205 (2002).

[23] L. Wang, L. Fu, and Y. Nie, J. Chem. Phys. **157**, 074502 (2022).

[24] The ensemble sizes N_{En} for the rapidly quenched system are: $N_{En} = 0.91 \times 10^6$ for $N = 196$; $N_{En} = 2.4 \times 10^6$ for $N = 786$; $N_{En} = 0.78 \times 10^6$ for $N = 1600$; $N_{En} = 0.11 \times 10^6$ for $N = 3200$; $N_{En} = 0.23 \times 10^6$ for $N = 30000$. For the annealed system they are: $N_{En} = 104\,000$ for $N = 1600$; $N_{En} = 46\,000$ for $N = 30000$.

[25] E. Flenner and G. Szamel, Nat. Commun. **6**, 7392 (2015).